Widespread nociceptive maps in the human neonatal somatosensory cortex.

Laura Jones[1†], Madeleine Verriotis*, Robert J. Cooper[2], Maria Pureza Laudiano-Dray[1], Mohammed Rupawala[1], Judith Meek[3], Lorenzo Fabrizi[1], & Maria Fitzgerald[1]

[1] Department of Neuroscience, Physiology & Pharmacology, University College London, London, WC1E 6BT, UK
[2] DOT-HUB, Department of Medical Physics & Biomedical Engineering, University College London, London, WC1E 6BT, UK
[3] Elizabeth Garrett Anderson Obstetric Wing, University College London Hospitals, London, WC1E 6DB, UK

*Current address: Department of Developmental Neuroscience, University College London Great Ormond Street Institute of Child Health, London, WC1N 1EH, UK

[†] Corresponding Authors: m.fitzgerald@ucl.ac.uk and laura.jones@ucl.ac.uk

Running title: Touch & pain topography in the human infant cortex
No. of Pages: 22
No. of Figures: 4
No. of Tables: 2
No. of words Abstract: 137
No. of words Introduction: 464
No. of words Discussion: 1714

Conflict of interest statement: RJC holds financial interests in Gowerlabs Ltd, who produce the device used in this study. The authors declare no other conflict of interest in this study.

Abstract

Topographic cortical maps are essential for spatial localisation of sensory stimulation and generation of appropriate task-related motor responses. Somatosensation and nociception are finely mapped and aligned in the adult somatosensory (S1) cortex, but in infancy, when pain behaviour is disorganised and poorly directed, nociceptive maps may be less refined. We compared the topographic pattern of S1 activation following noxious (clinically required heel lance) and innocuous (touch) mechanical stimulation of the same skin region in newborn infants (n=32) using multi-optode functional near-infrared spectroscopy (fNIRS). Within S1 cortex, touch and lance of the heel elicit localised, partially overlapping increases in oxygenated haemoglobin concentration ($\Delta[HbO]$), but while touch activation was restricted to the heel area, lance activation extended into cortical hand regions.   The data reveals a widespread cortical nociceptive map in infant S1, consistent with their poorly directed pain behaviour.

Introduction

Somatotopically organised cortical maps of activity evoked by innocuous or noxious mechanical stimulation allow us to localise our sense of touch or pain (Penfield and Boldrey, 1937; Harding-Forrester and Feldman, 2018), and may also convey computational advantages in the relay of afferent information to higher brain areas (Thivierge and Marcus, 2007). In adults, overlapping regions are involved in the cortical processing of noxious and innocuous mechanical stimulation (Kenshalo et al., 2000; Lui et al., 2008) and detailed fMRI analysis reveals a fine-grained somatotopy for nociceptive inputs in primary somatosensory cortex (SI) that are aligned with activation maps following innocuous tactile stimuli, suggesting comparable cortical representations for mechanoreceptive and nociceptive signals (Mancini et al., 2012).

A whole-body topographical map of innocuous mechanical stimulation develops in the sensorimotor cortices over the early postnatal period in rats, which represent the human final gestational trimester (Seelke et al., 2012). Distinct representations of the hands and feet can be observed from 31 weeks using fMRI (Dall'Orso et al., 2018), becoming increasingly localised by term age (Allievi et al., 2016). While haemodynamic responses to a clinically-required heel lance have been recorded from 28 weeks using functional near-infrared spectroscopy (Slater et al., 2006) and can be distinguished from innocuous tactile evoked brain activity in EEG recordings from 34-35 weeks (Fabrizi et al., 2011), the source of this activity and topographic representation of these two modalities have not been mapped, or their alignment established, in the infant cortex.

Infant pain behaviour is exaggerated and disorganised in newborn rodents and human infants (Fitzgerald, 2005, 2015; Cornelissen et al., 2013). Poor spatial tuning of nociceptive reflexes and receptive fields is a feature of the developing somatosensory system, followed by the emergence of adult organisation through activity-dependent refinement of synaptic connections (Beggs et al., 2002; Schouenborg, 2008; Koch and Fitzgerald, 2013).   We hypothesised that this developmental process is reflected in ascending nociceptive signals to SI, leading to widespread S1 activation and poor spatial localisation of noxious events in early life.

To test this hypothesis, we used multioptode functional near-infrared spectroscopy (fNIRS) to map nociceptive and innocuous mechanoreceptive activity across the infant sensorimotor cortex. fNIRS is a non-invasive measure of cerebral haemodynamic changes which can be performed at the bedside, while in skin-to-skin holding and in a naturalistic hospital setting during clinically required procedures. Using the temporal and spatial profiles of haemodynamic responses to a noxious heel lance and an innocuous touch of the hand and the heel, we show that haemodynamic activity elicited by noxious and innocuous mechanical stimuli have partially overlapping topographies in the human infant S1 cortex but that the two maps are not aligned. Noxious stimulation of the heel in the newborn evokes more widespread S1 activation than innocuous stimulation, that extends into inferior regions, normally associated with representation of the hand.

Results

Innocuous hand and heel touch evoked activity is somatotopically organised in the newborn infant S1 cortex

We first established the cortical topography of touch activation in newborn infants by mapping the extent of activation in the contralateral somatosensory (S1) cortex following innocuous mechanical stimulation (touch) of the hand and heel. **Figure 1a** and **1b** show a significant and localised increase in average concentration of oxygenated haemoglobin ($\Delta[HbO]$) in contralateral optode channels following touch of each body area (n=11, hand touch; n=16 heel touch).   Touch stimulation of the hand elicited significant increases in seven channels, with a maximum change (0.33 μM at 9.2 s post-stimulus) at the channel corresponding to the FCC5 position of the 10:5 placement system (Oostenveld and

2

104 Praamstra, 2001), while touch of the heel elicited significant increases in seven channels,
105 with a maximum change (0.35 µM at 15.8 s) at the channel corresponding to the CPP1 10:5
106 position.
107 The somatotopically localised increases in Δ[HbO] were accompanied by a widespread
108 decrease in Δ[Hb] over the whole peri-rolandic area (hand: significant decreases in eight
109 channels [peak change: -0.18 µM at 17.6 s]; heel: significant decreases in 14 channels [peak
110 change: -0.21 µM at 11.1 s]). An inverse response (significant decrease in Δ[HbO],
111 significant increase in Δ[Hb], or both) was mostly restricted to channels surrounding the
112 hand and foot areas of the S1, respectively. Individual channel data is shown in **Figure 1 –**
113 **Source Data 1**.
114
115
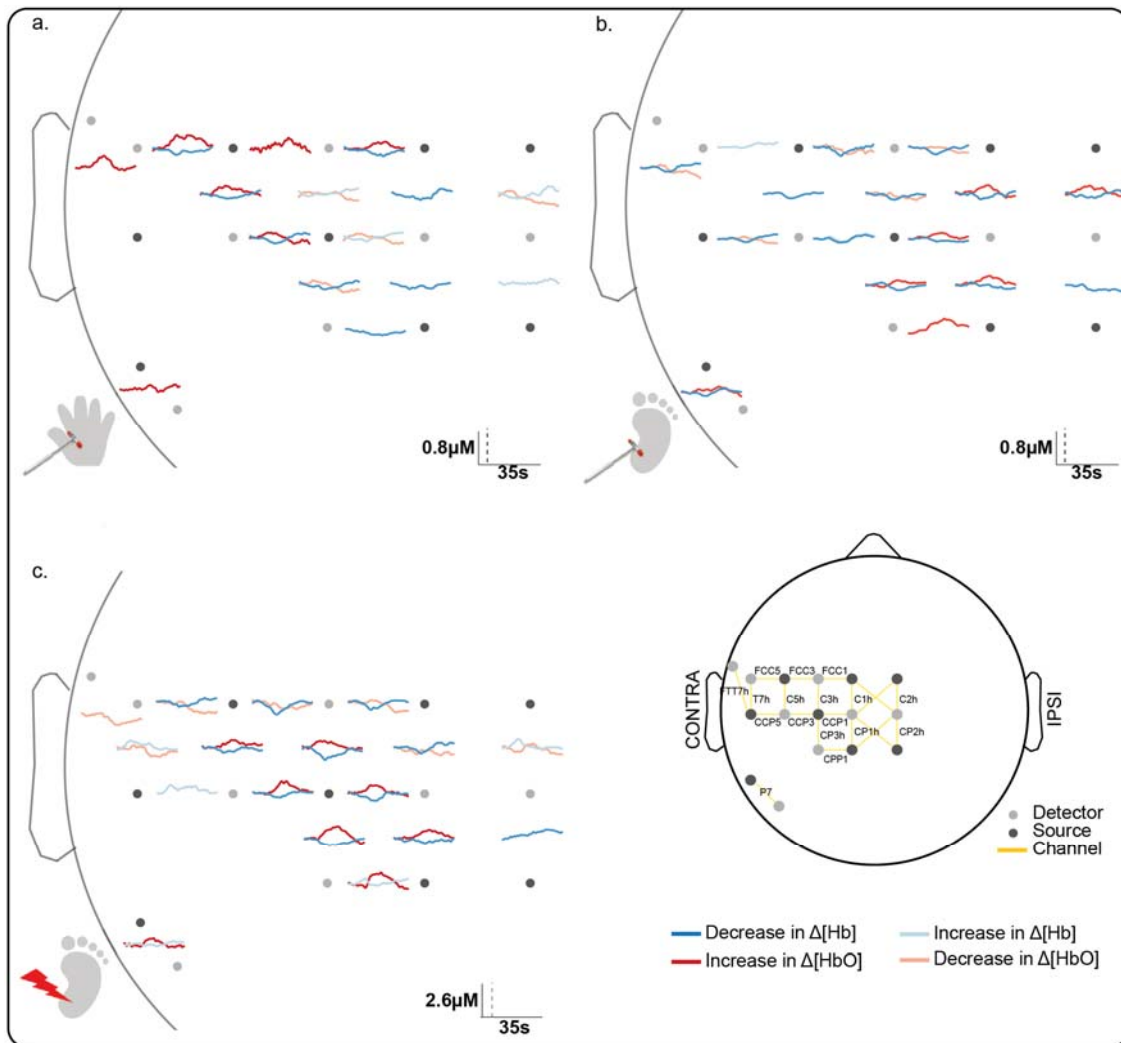
116
117 **Figure 1. Significant channel-wise haemodynamic response following innocuous**
118 **(touch) and noxious (lance) mechanical stimulation of hand and heel.** *Average*
119 *significant change in* concentration of oxygenated *(Δ[HbO]) (red) and deoxygenated*
120 *haemoglobin (Δ[Hb]) (blue) during (a) hand touch (n=11), (b) heel touch (n=16) and (c) heel*
121 *lance (n=11). Channels with significant increases in Δ[HbO] and decreases in [Hb] (i.e.*
122 *canonical response) during the activation period are shown with solid dark lines, channels*
123 *with an inverse response only (decrease in Δ[HbO] and increase in Δ[Hb]) are shown with*
124 *pale solid lines. Note the difference in the scale bar between touch and lance. The*

3

125   *equivalent plots for non-significant changes are shown in* **Figure 1 - figure supplement 1**
126   *and details of individual channel responses are in* **Figure 1 – Source Data 1.**
127
128   Image reconstruction of the channel data (Figure 2a and 2b) shows that the topography of
129   touch peak activation in the newborn infant S1 is consistent with the known adult S1
130   topography: the area representing the foot lies in the superomedial postcentral gyrus, while
131   the area for the hand is more lateral and inferior (Penfield and Boldrey, 1937; Harding-
132   Forrester and Feldman, 2018; Willoughby et al., 2020).
133

Noxious lance of the heel elicits widespread activation extending into inferior SI

135   We next mapped activation in the contralateral S1 following a noxious, clinically required,
136   lance stimulus to the heel in newborn infants. The average channel response (**Figure 1c**)
137   and the image reconstruction (**Figure 2c**) show the significant and widespread increase in
138   Δ[HbO] following the heel lance, which extends beyond the somatotopic area for heel touch
139   to encompass inferior areas of SI, which were associated with touch of the hand.
140   Heel lance elicited significant increases in Δ[HbO] in eight channels, with a maximum
141   increase (0.96 µM at 14.5 s) at the channel corresponding to the CP3h 10:5 position. Four
142   of the channels with a significant increase in Δ[HbO] following the lance, also had a
143   significant increase in Δ[HbO] following touch of the heel. Notably two channels also
144   displayed a significant increase following touch of the hand. Demonstrating a topographic
145   overlap with both the hand and heel touch responses. The accompanying decrease in
146   concentration of deoxygenated haemoglobin (Δ[Hb]) was widespread (significant decreases
147   in 11 channels; peak change 1.03 µM at 9.1 s), and an inverse response was found in all
148   channels surrounding those with a canonical response (**Figure 1c and 2c**).
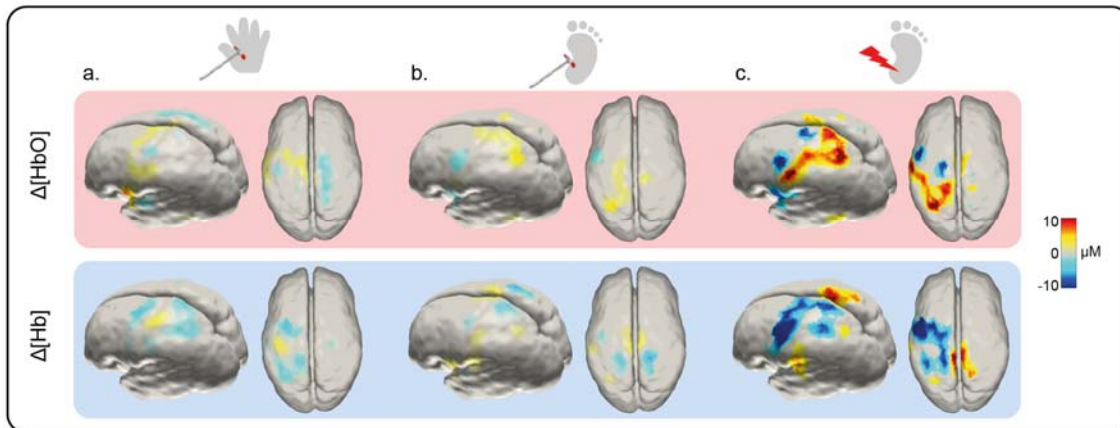
149
150   **Figure 2. Image reconstruction at peak latency of the Δ[HbO] and Δ[Hb] response to**
151   **an innocuous (touch) and noxious (lance) mechanical stimulation of hand and heel.**
152   *Significant changes (compared to baseline) in* concentration of oxygenated *(Δ[HbO]) (top*
153   *row) and d*eoxygenated haemoglobin *(Δ[Hb]) (bottom row) following (a) hand touch (n=11),*
154   *(b) heel touch (n=16) and (c) heel lance (n=11).*
155

Newborn infant nociceptive maps are more widespread and not somatotopically aligned with innocuous mechanoreceptive maps

158   We then compared the responses to heel touch and lance in terms of amplitude, latency and
159   position of peak change, and extent and overlap of the overall areas of activation at peak
160   latency. Heel touch and lance elicited a peak increase in Δ[HbO] at the same latency and
161   location (distance between peaks = 1.65mm, p=.156; difference in peak latency = 2 s [14 vs
162   16 s], p=.358; Figure 3a-b), however this was significantly larger (maximum Δ[HbO]: 16.06
163   vs 5.43 µM, p=.001) and wider (FWHM area: 51.41 vs 43.79 mm^2, p=.019) following lance

4

164 stimulation. The overall area of activation was also significantly more widespread following
165 heel lance (Δ[HbO] overall area: 455.27 vs 259.51 mm², p=.009) and only partially
166 overlapped to that following touch (Figure 3a). The increase in Δ[HbO] was significantly
167 larger following lance compared to touch across 50% of the lance-only activation area
168 (Figure 3a – red area, Figure 3c) and across 26% of the overlap area (Figure 3a – orange
169 area, Figure 3c). However, there was no significant difference in Δ[HbO] changes between
170 lance and touch across the touch-only activation area (Figure 3a – pink area). This shows
171 that the significantly larger and wider peak response and more widespread overall area of
172 activation following lance is not due to a greater systemic hemodynamic change following
173 this stimulus.
174 The location, but not latency, of the peak change in Δ[Hb] was significantly different following
175 heel touch and lance (distance between peaks = 51.88mm, p=.041; difference in peak
176 latency = -19.3 s [9.5 vs 28 s], p=.028), which was also significantly larger (maximum Δ[Hb]:
177 -22.54 vs -6.62 µM, p<.001) and wider (Δ [Hb] FWHM area: 15.31 vs 4.63 mm^2, p<.001)
178 following heel lance (Figure 3, Figure supplement 1). The overall area of activation was also
179 significantly more widespread following heel lance (Δ[Hb] overall area: 475.24 vs 95.53 mm²,
180 p<.001). The key difference between the two patterns of activation is that the heel touch
181 Δ[HbO] response is limited to the areas of the S1/M1 associated with the foot, whereas the
182 lance Δ[HbO] response extends towards other more ventral regions of S1.
183

184

5
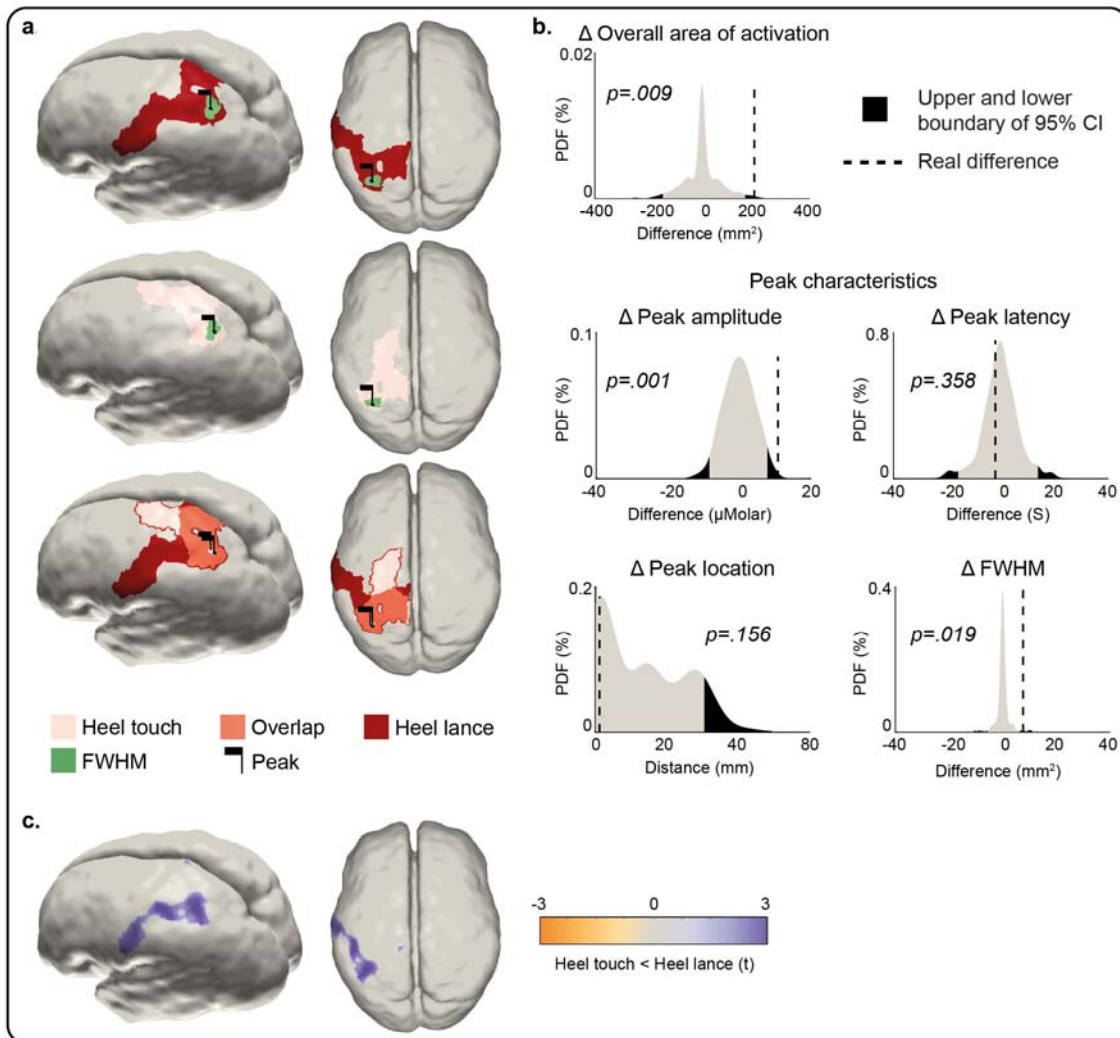
185 **Figure 3. Comparison of the peak and area of activation of the ∆[HbO] response to an**
186 **innocuous (touch) and noxious (lance) mechanical stimulation of the heel.** (*a) Overall*
187 *area of significant changes in concentration of oxygenated haemoglobin (∆[HbO]) following*
188 *heel lance (red), heel touch (pink) and both (orange). Black flags demark the location of*
189 *peak changes and green areas the extent of their full-width half-maximum (FWHM). (b)*
190 *Statistical position of real differences between heel touch and lance in peak amplitude,*
191 *FWHM, latency and location, and overall area of activation in respect to non-parametric null*
192 *distributions obtained with bootstrapping and phase scrambling. (c) Comparison of*
193 *response magnitude at each node. Results show the t-statistic at significantly different nodes*
194 *within the areas of activation shown in (a). The equivalent plots for ∆[Hb] are shown in*
195 ***Figure 3 - figure supplement 1*** *and* ***Figure 3 - source data 1***.

196

197 ## Discussion

198 ***A widespread nociceptive topographic map in infant S1 that overlaps but is not***
199 ***aligned to the innocuous mechanoreceptive map***

200 Somatosensory maps of cortical activity evoked by a cutaneous tactile or noxious stimulus
201 provide a framework for localising the sense of touch or pain (Treede et al., 1999; Thivierge
202 and Marcus, 2007). The adult primate S1 has a defined somatotopic organization of tactile
203 and nociceptive cortical receptive fields (Andersson et al., 1997; Kenshalo et al., 2000)
204 including spatially precise cortical maps of Aδ and Aβ afferent fibre input (Chen et al., 2011).
205 Human fMRI studies show that adult somatotopic maps of noxious and non-noxious
206 mechanical stimulation substantially overlap (Lui et al., 2008) and detailed analysis reveals a
207 fine-grained somatotopy for nociceptive inputs in primary somatosensory cortex (S1) that are
208 highly aligned with maps of innocuous tactile stimuli, suggesting comparable cortical
209 representations for mechanoreceptive and nociceptive signals (Mancini et al., 2012). Here
210 we have shown that this comparable representation is not present in the newborn infant S1
211 cortex.

212 Noxious mechanical stimulation evokes a larger peak increase in concentration of
213 oxygenated haemoglobin (∆[HbO]) and decrease in concentration of deoxygenated
214 haemoglobin (∆[Hb]) compared to innocuous stimulation of the same body area at
215 comparable location and latency as reported elsewhere (Bartocci et al., 2006; Slater et al.,
216 2006; Verriotis et al., 2016b). The fact that the noxious activation is greater than the touch
217 evoked activity is presumably due to hyperaemia associated with greater depolarisation and
218 spike activity within the activated areas. However, it does not explain the differing
219 topography of the overall are of activation reported here. Although a lance, being a more
220 intense stimulus, could be thought to cause more widespread cortical activation throughout
221 the cortex, here the response to the lance is only significantly larger than touch in 50% of
222 lance-only area of activation, 26% of the lance and touch overlap area, and nowhere in the
223 touch-only activation area. Our results instead suggest that the response to a noxious and
224 innocuous mechanical stimulus are not spatially aligned. Within S1 itself, the infant has a
225 distinct somatotopic map for touch, similar to that described in adults, with the area
226 representing the foot lying in the superomedial postcentral gyrus, and the area for the hand
227 located more inferiorly (Penfield and Boldrey, 1937; Blake et al., 2002; Akselrod et al.,
228 2017), consistent with previous reports in newborn infants (Dall'Orso et al., 2018). Noxious
229 heel lance, on the other hand, evokes widespread activity within S1, peaking in a similar
230 area of the superomedial postcentral gyrus as touch activity, but extending to the hand
231 representation area. All stimuli elicited a significant response in the control channel which
232 may suggest that the responses extended more posteriorly to S1, nevertheless, our data
233 shows that the S1 somatotopic nociceptive map is not as precise as the touch map in the
234 newborn.

235 It should be noted that fNIRS is an indirect measure of neuronal activation and may be
236 confounded by systemic vascular changes such as increases in blood pressure, which may

237 be more likely following a noxious versus innocuous stimulus. However, we removed global
238 changes common across channels using PCA, and our results point to misaligned noxious
239 and innocuous activity, with widespread noxious activity across the S1 specifically, but not
240 the whole cortex as one would expect following systemic changes. Several channels/nodes
241 did not show a significant response following the heel lance compared to baseline, and the
242 heel lance did not have a greater response compared to heel touch at every node. Together,
243 these findings suggest that the greater magnitude of the heel lance response is not due to
244 systemic changes elicited by the noxious stimulus. However, as fNIRS (as with fMRI) is a
245 measure of the vascular response following neuronal activity, the precise degree of
246 localisation of either neuronal response is limited.
247
248 *Measuring the cortical haemodynamic response to innocuous and noxious*
249 *mechanical stimulation in neonates*
250 fNIRS is ideally suited to a study of this kind as recording and sensory stimulation, including
251 clinically required heel lance, can be performed at the infant cotside (Bartocci et al., 2006;
252 Slater et al., 2010; Kashou et al., 2016; Verriotis et al., 2016b). Other methods of measuring
253 this either do not provide sufficient spatial information and source localisation, such as EEG
254 recording of nociceptive-related ERPs (Fabrizi et al., 2011; Jones et al., 2018) or are limited
255 by the use experimental 'pinprick' stimulators, that for ethical reasons are not actually
256 painful, such as in fMRI studies (Goksan et al., 2015).
257 The change in the Δ[HbO] and Δ[Hb] following sensory stimulation is an indirect measure of
258 neural activity: simultaneous vertex EEG and fNIRS recordings over S1 show that
259 haemodynamic and neural responses are related in magnitude (Verriotis et al., 2016b).
260 Following all stimuli, and consistent with the mature canonical response, channels showing a
261 significant increase in Δ[HbO] also had a smaller decrease in Δ[Hb]. Regional overperfusion
262 following neuronal activation, beyond that required by metabolic demands, means that less
263 Hb is removed from the region compared to the oversupply of HbO. However, the decrease
264 in Δ[Hb] was more widespread (but smaller in magnitude) compared to the localised
265 increase in Δ[HbO]. This type of response, not previously reported in infants (de Roever et
266 al., 2018), suggests that more blood is leaving the region (removing Hb) compared to the
267 incoming supply (no significant change in Δ[HbO] in peripheral channels) due to immature
268 regulation of cerebral blood flow (CBF). There are multiple mechanisms by which blood
269 vessels dilate and CBF increases following neural activation, including arterial CO_2 and O_2
270 concentrations, which relax/contract the smooth muscle cells of cerebral arteries and
271 arterioles (Kety and Schmidt, 1948), and astrocyte and pericyte activity which controls
272 vessel diameter and the propagation of vasodilation along the vascular tree (Takano et al.,
273 2006; Cai et al., 2018), many of which are still developing in the newborn (Pryds and
274 Greisen, 1989; Binmöller and Müller, 1992; Fujimoto, 1995) leading to rapid changes in CBF
275 over the first postnatal days as cerebral circulation adapts (Meek et al., 1998).
276 The infants in this study were held skin to skin, swaddled in their mother's arms in a
277 naturalistic setting, which is a major advantage of fNIRS recording over fMRI for human
278 developmental studies of brain function. Video recording and investigator scoring confirmed
279 that while some infant movement and maternal touching did take place and that some
280 babies did move following the lance, these movements spanned different body parts and
281 latencies such that any associated cortical response would be cancelled during the
282 averaging process. Indeed, comparison of the time-series following heel touch with and
283 without removing trials with known movement, showed no significant difference (Figure 1,
284 Figure supplement 2). Furthermore, 33-50% of babies did grimace for up to 7 seconds
285 following the lance, but if these facial movements mediated the response following the lance,
286 this would have prolonged the peak or duration of the change in [HbO], while in fact the
287 latency and time course of the response to both stimuli was the same (see Figure 1).
288

7

Differential development of somatosensory and nociceptive topographic maps

A whole-body topographical map of innocuous mechanical stimulation develops in the sensorimotor cortices over the early postnatal period in rats (Seelke et al., 2012), which represents the human final gestational trimester. In humans, distinct representations of the hands and feet can be observed from 31 weeks gestation, using fMRI (Dall'Orso et al., 2018), and from 28 weeks using neural activity recorded from the scalp (Donadio et al., 2018; Whitehead et al., 2018, 2019). The response to innocuous mechanical stimulation was more localised in S1 than the wider and less refined topographical map of noxious mechanical stimulation, suggesting a slower maturation of the S1 circuitry involved in nociceptive processing compared to touch processing in the infant brain.

In rodents, at every level of the developing somatosensory central nervous system, tactile processing matures before nociceptive processing (Fitzgerald, 2005; Koch and Fitzgerald, 2013; Chang et al., 2016, 2020; Verriotis et al., 2016a) consistent with a delayed refinement of a cortical nociceptive map.   Widespread nociceptive cortical maps are consistent with infant pain behaviour, characterised by exaggerated and disorganised nociceptive reflexes in both rodent pups and human neonates (Fitzgerald, 2005, 2015), and which can fail to remove a body part from the source of pain (Waldenström et al., 2003).   Nociceptive reflexes following noxious heel lance are larger in magnitude and significantly more prolonged in human infants compared to adults (Cornelissen et al., 2013) and have widespread cutaneous receptive fields that encompass the whole lower limb (Andrews and Fitzgerald, 1994). This lack of organisation could be reflected in the ascending spinothalamic and thalamocortical projections, delaying the maturation of S1 cortical nociceptive maps in the newborn. Topographic maps are established and aligned via multiple mechanisms, including molecular cues, spontaneous or sensory-dependent remodelling, and refinement. Initially, somatosensory maps are diffuse and overlapping, but in the rodent somatosensory cortex, excitatory thalamocortical afferents undergo activity-dependent refinement to sharpen these maps (Iwasato et al., 1997). Equally important is the maturation of inhibitory interneuron sensory maps which, in contrast, expand over development in an experience dependent manner (Quast et al., 2017). Slow developmental broadening of an inhibitory nociceptive network may explain the widespread nociceptive map in S1 and also the greater amplitude of EEG noxious responses in infants compared to adults (Fabrizi et al., 2016).

Pain and the developing S1 cortex

This study highlights the importance of understanding the development of touch and pain processing in the human infant brain.   The widespread S1 nociceptive topography discovered here implies that the infant S1 cortex would be unable to accurately localise noxious events and may lack the computational ability to reliably send noxious information to higher brain centres (Thivierge and Marcus, 2007; Harding-Forrester and Feldman, 2018). Heel lance is one of many skin-breaking procedures commonly performed in neonatal hospital care (Laudiano-Dray et al., 2020) and this study reveals the extent of cortical activation that follows just one such noxious procedure in the newborn. This contrasts with innocuous mechanical stimulation, such as touch, which activates a spatially restricted and somatotopically defined cortical area.   Increasing evidence that repeated noxious experiences have adverse effects upon the developing brain (Ranger and Grunau, 2014; Duerden et al., 2018), underlines the importance of these results and the need for a better understanding of the mechanisms underlying the maturation of cortical nociceptive topographic maps.

Materials and Methods
Participants

8

Thirty-two infants (35-42 gestational weeks at birth, 0-7 days old, 12 female; **Table 1**) were recruited from the postnatal, special care, and high dependency wards within the neonatal unit at University College London Hospital. Infants received either 1) innocuous mechanical stimulation (touch) of the heel, 2) innocuous mechanical stimulation of the hand, or 3) a noxious mechanical stimulation (clinically required lance) of the heel. Six infants received touch stimulation of both the heel and hand. This sample size is sufficient as similar high impact works using single trial noxious stimulation or multiple mechanical stimulations have yielded significant results with group sample sizes of 5-15 (Bartocci et al.,2006) and 10-15 (Arichi et al., 2012), respectively. Ethical approval for this study was given by the NHS Health Research Authority (London – Surrey Borders) and the study conformed to the standards set by the Declaration of Helsinki. Informed written parental consent was obtained before each study.

Table 1. Infant demographics. Demographic information about the subjects that received tactile and noxious stimuli of heel and hand.

|	Heel lance	Heel touch	Hand touch	p
N	11	16	11	
GA (weeks^{+days})	39^{+2} ($35^{+2} - 41^{+5}$)	39^{+4} ($35 - 42^{+3}$)	39^{+2} ($37^{+5} - 41^{+3}$)	.287
PNA (days)	4 (0 - 7)	3 (0 - 6)	3 (0 - 4)	.115
Females	4 (36%)	6 (38%)	5 (45%)	.889
Birth weight (g)	3134 (2220 - 4072)	3250 (2360 - 4080)	3300 (2450 - 3754)	.774
Caesarean deliveries	2 (18%)	8 (50%)	3 (27%)	.196
Head circumference (cm)	34 (32 – 35.5)	34.25 (31 - 37)	34 (32.5 - 36)	.900

Values represent median and range or proportion. GA = gestational age (weeks from the first day of the mothers last menstrual cycle to birth); PNA = postnatal age (days since birth). No significant difference was found in any demographic parameter across the three groups (one-way ANOVA results in the last column).

Experimental design
Brain activity (fNIRS) was recorded following a noxious (clinically-required heel lance) or innocuous (touch) mechanical stimulation of the limbs at the bedside in the neonatal unit.

Functional Near-Infrared Spectroscopy recording
Infants wore a 21-channel array consisting of 8 sources and 8 detectors with inter-optode distances of 2.5-4 cm. The array was secured over the pericentral area of the scalp on the side contralateral to the stimulation with a custom designed textile cap (EasyCap, **Figure 4a**). The infants' head circumference, ear to ear lateral semi-circumference, and nasion to inion distance were measured and the cap was placed on the head by aligning specific 10/5 locations (Cz, T7). This optode arrangement provided sensitivity coverage for the somatomotor cortex contralateral to the stimulation site and of the medial part on the ipsilateral side (**Figure 4d**). One source-detector pair was placed at a more ventral posterior location of the scalp (P7 of the international 10/5 positioning system) (**Figure 4b**). This channel was sensitive to the posterior temporal lobe and worked as a control channel (**Figure 4b-d**). A continuous wave recording system was used with 2 wavelengths of source light at 780nm and 850nm and a sampling rate of 10Hz to measure changes in oxy- and deoxy-haemoglobin concentration (Gowerlabs NTS fNIRS system).
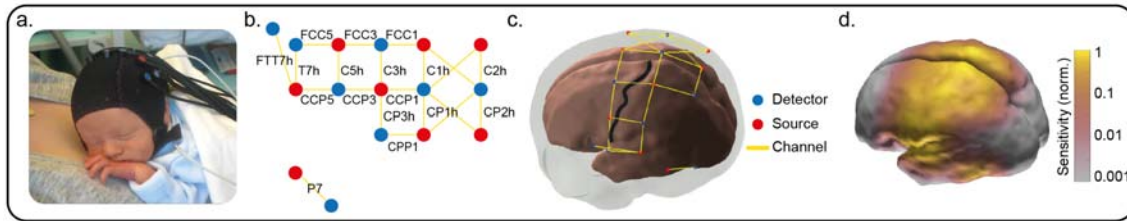
Figure 4. Optode locations and sensitivity map *(a) Typical fNIRS set up on a neonate of 35^{+2} weeks GA, 7 dys PNA. (b) Channel locations according to the international 10-5 placement system (Oostenveld and Praamstra, 2001). Names of four diagonal channels (channels overlaying Cz and CPz) are not included as these were omitted from the analysis due to low signal to noise ratio. (c) Locations of the fNIRS sources, detectors and resulting measurement channels registered to a 39-week anatomical atlas. The central sulcus has been highlighted with a black line and the location of S1 is the gyrus posterior to this sulcus. (d) Normalized fNIRS sensitivity illustrating the spatial coverage provided by the channel arrangement in panel (c). This sensitivity map was calculated using the photon measurement density functions derived from the TOAST++ light transport modelling package.*

Noxious mechanical stimulation

The noxious stimulus was a clinically required heel lance for blood sampling. Blade release was time-locked to the NIRS recording using an accelerometer attached to the lancet (Worley et al., 2012). The lancet was placed against the heel for at least 30s prior to the release of the blade. This was to obtain a baseline period free from other stimulation. The heel was then squeezed 30s after the release of the blade, again to ensure a post-stimulus period free from other stimuli. All lances were performed by the same trained nurse (MPL-D) using a disposable lancet, and standard hospital practice was followed at all times.

All infants were prone against their mother's chest. The mother, who was inclined on a chair or bed, was instructed to avoid moving or stimulating the infant during the 1 minute before and after the release of the lance.

Innocuous mechanical stimulation

Innocuous mechanical stimulation was delivered by light touch on the lateral edge of the infants' palms and/or heels using a hand-held tendon hammer (ADInstruments). A piezo-electric sensor mounted on the hammer head provided a synchronising signal to the NIRS recording. A train of up to 15 touches (average = 11.1) was delivered to each limb with a variable inter-stimulus interval of 35 – 60 seconds. This resulted in an average of 11.5 heel touches (range = 7 – 15) and 10.6 hand touches (range = 6 – 13) per infant. Stimulus repetition did not cause habituation of the response to touch (no significant difference in the average time series between the first and last 50% of the trials).

Infant movement

To limit cortical activation not related to the investigated sensory stimuli, body movements were minimized during the lance procedure, as infants were swaddled (wrapped securely in clothes/blankets) against the mother's chest and the research nurse was holding the exposed foot throughout the period before and after the stimulus.

Infant movements, or maternal handling were recorded on video, which was synchronised with the NIRS recording using an LED light within the frame that was activated by the release of the lance (Worley et al., 2012) or annotated at the time of study using a stopwatch. For lance trials, movements or maternal handling were separated into body parts and coded per second as either 0 (not present) or 1 (present) for the 30 s post-stimulus (Table 2). Following the lance, 2 babies did not move, 5 babies made small movements

10

427 (including: small or brief grimace, head nod, twitch, small hand movement), 4 babies made
428 larger movements (including arms, large or prolonged grimace, nod of head), and 2 babies
429 received tactile stimulation from the mother (including: positioning the head, stroking the
430 face). Following touch, body movement were present in an average of 2.9 trials in 8/16
431 infants (heel) and 1.4 trials in 11/11 infants (hand). Although every effort was made to
432 minimize trials affected by body movements, these were sometimes unavoidable following a
433 single lance trial and therefore were include for both lance and touch analysis. However, this
434 is unlikely to have affected our results because body movements were not systematically
435 associated to the stimulus of interest as they spanned different body parts and latencies
436 such that any associated cortical response would be cancelled during the averaging
437 process. Indeed, comparison of the time-series following heel and hand touch with and
438 without removing trials with known movement, showed no significant difference (Figure 1 –
439 Figure supplement 2).

440

441 **Table 2**. **Infant movements.** The number of infants who displayed movements or received
442 tactile stimulation from their mother each second in the 30s following lance.

Number of infant and maternal movements

Post-lance (s)	Hand	Head	Face	Foot	Arm	Mother touching face	Mother touching head
1	1	1	4	0	2	1	1
2	1	1	6	1	2	1	1
3	1	0	6	1	2	1	1
4	1	0	6	0	2	1	1
5	1	1	6	0	2	1	1
6	1	1	6	0	2	1	0
7	0	1	4	0	1	1	0
8	0	1	3	0	1	1	0
9	0	1	2	0	1	1	0
10	0	0	1	0	1	1	0
11	0	0	1	0	1	1	0
12	0	0	1	0	1	1	0
13	0	0	1	0	1	1	0
14	0	0	1	0	1	1	0
15	0	0	1	0	0	1	0
16	0	0	1	0	0	1	0
17	0	0	0	0	0	1	0
18	0	0	0	0	0	1	0
19	0	0	0	0	0	1	0
20	0	0	0	0	0	1	0
21	0	0	0	0	0	1	0
22	0	0	0	0	0	1	0
23	0	0	0	0	0	1	0
24	0	0	0	0	0	1	0
25	0	0	0	0	0	1	0
26	0	0	0	0	0	1	0
27	0	0	0	0	0	1	0
28	0	0	0	0	0	1	0
29	0	0	0	0	0	1	0
30	0	0	0	0	0	1	0

443

444 *Each movement or stimulation was scored as present (1) or not present (0) per infant, and*
445 *the value in each cell represents the total number of infants (out of 11) for whom each*
446 *movement or stimulation was observed.*
447

Data pre-processing

449 All data were pre-processed in Homer2 (Huppert and Boas, 2005). The 4 channels crossing
450 over the midline had consistent poor signal quality (light intensity < 0.01, SNR < 2) and were
451 not considered further (**Figure 4b and 4c)**. Recordings from 1-8 (average: 0.74) channels in
452 11 (29%) trials were also removed for lance and touch stimuli. Data were then converted into
453 optical density, motion artefacts were detected (change in amplitude > 0.7 and/or change in
454 standard deviation > 15 over a 1s time period) and then corrected using Wavelet filtering
455 (Molavi and Dumont, 2012). Instrumental drift and cardiac artefact were removed with a
456 0.01-0.5 Hz bandpass filter. Optical density changes recorded from all channels (likely
457 related to stimulus dependent systemic physiological changes) were removed using
458 Principal Component Analysis ((Kozberg and Hillman, 2016; Tachtsidis and Scholkmann,
459 2016); 1 component removed for every subject). Finally, data were converted into changes
460 in oxy- and deoxy-haemoglobin concentration (Δ[HbO] and Δ[Hb]) using the modified Beer–
461 Lambert law (Delpy et al., 1988) with a differential path-length factor of 4.39 (Wyatt et al.,
462 1990). The continuous signal was then epoched from -5 to 30 s around the noxious and
463 somatosensory stimuli. Somatosensory stimuli were averaged for each subject.
464

Signal to Noise

466 The signal to noise ratio (SNR) for lance and for touch were calculated. Despite the peak
467 signal for lance being larger, the estimated SNR of the peak was lower, because more touch
468 trials were averaged in this study: $\frac{(Peak_{Lance}*\sqrt{N_{Lance}})}{(Peak_{Touch}*\sqrt{N_{Touch}})}$ = ratio of lance to touch SNR;

469 $\frac{(0.96*\sqrt{11})}{(0.35*\sqrt{184})} = 0.67$.

470

Channel-wise data analysis

472 Pre-processed data were then averaged across trials for each subject (except lance which
473 only had one trial) and analysed using custom MATLAB scripts (Mathworks; version 16b).
474 For each channel, significant changes in Δ[HbO] and Δ[Hb] were identified with a two-tailed
475 t-test (α = 0.01) comparing each time point post-stimulus against the baseline. This baseline
476 distribution was calculated as the mean of the individual baselines (-5 – 0s before stimulus)
477 according to:

$$\frac{1}{S}\sum_{i=1}^{S} x_i \sim N\left(\frac{1}{S}\sum_{i=1}^{S} \mu_i, \frac{1}{S^2}\sum_{i=1}^{S} \sigma_i^2\right).$$

478 Where S is the number of subjects and $x_i \sim N(\mu_i, \sigma_i^2)$ is the baseline for subject i.
479 Bonferroni correction was used for multiple comparisons (17 channels x 300 samples = 5100
480 comparisons). Only changes (increases or decreases) which were continuously significant
481 for at least 1 second (10% of the length of the post-lance period) were retained (Guthrie and
482 Buchwald, 1991).
483

Data analysis in image space

485 <u>Image reconstruction</u>
486 The channel-wise data was used to create functional images using a cortically constrained
487 linear reconstruction approach at each time-point to obtain image time-series for each
488 subject. The fNIRS array was registered to a 39-week gestational age anatomical mesh
489 model with 784391 nodes (Brigadoi et al., 2014) using tools from the AtlasViewer package

490 (Aasted et al., 2015). Images were reconstructed using the DOT-HUB toolbox
491 (www.github.com/DOT-HUB) and the TOAST++ light transport modelling package
492 (Schweiger and Arridge, 2014) (www.github.com/toastpp), with zeroth-order Tikhonov
493 regularization with a regularization hyperparameter of 0.1.

494 <u>Assessment of peak changes in Δ[HbO] and Δ[Hb]</u>
495 Image space analysis was conducted separately from channel space. We first assessed if
496 hand and foot touch and foot lance evoked a significant response in Δ[HbO] and Δ[Hb], by
497 comparing their peak change to baseline. To do that, we averaged the image time-series
498 and found the latency at which the maximum change occurred anywhere across the cortex.
499 For each node, significant changes at that latency in Δ[HbO] and Δ[Hb] were assessed with
500 a two-tailed t-test (α = 0.01) comparing the 5-second window around the identified peak
501 latency against the 5-second baseline. As in channel-wise analysis peak signal and baseline
502 distributions were estimated by concatenating the individual baselines (-5 – 0s pre-stimulus)
503 and peak windows (-2.5 – 2.5s around peak latency). Bonferroni correction was used for
504 multiple comparisons (784391 nodes = 784391 comparisons). To display these results we:
505 (1) reconstructed an image using the average channel-wise data within the 5-second
506 window around the peak latency (averaged in time) for hand touch, heel touch and lance
507 and (2) masked this image according to the result of the statistical test above.

508 <u>Comparison of peak changes in Δ[HbO] and Δ[Hb] between heel lance and touch</u>
509 Next, we compared the significant changes in Δ[HbO] and Δ[Hb] between the heel lance and
510 touch conditions in two ways: 1) comparing the magnitude of the response at peak latency at
511 every node using a student's t-test, 2) comparing the characteristics of the peak response
512 (overall area of activation and latency, location, and spread of the peak change in Δ[HbO]
513 and Δ[Hb]) using a non-parametric test.

514 Overall area of activation was defined by starting at the node with the peak change and
515 continually expanding to include neighbouring nodes that were (1) connected by 3 face
516 edges, and (2) had a significant change from baseline. Difference in peak location was the
517 Euclidean distance between the peaks. Spread of the peak was defined as the part of the
518 overall area of activation around the peak where changes in Δ[HbO] (or Δ[Hb]) were at least
519 half of the peak change (full-width half-maximum, FWHM).

520 The non-parametric null distribution was derived by calculating these differences between
521 randomly selected sets of surrogate image time-series (bootstrapping on surrogate data).
522 We here describe how we obtained surrogate image time-series and then how we
523 conducted bootstrapping.

524 Each individual recording (i.e image time-series) can be considered as the linear sum of a
525 signal of interest (i.e. the response to the stimulus) and a stationary random noise
526 component. The assumption is that the signal is the same in each recording while the noise
527 changes (van Drongelen, 2007). Therefore, if we were to conduct another recording on
528 another subject the new data would be the linear sum of the *same* signal that we find in the
529 original data but *different* random noise. Creating surrogate data consists in generating new
530 random noise to add to the signal estimated from our data. To do this we: (1) estimate the
531 signal by averaging across individual recordings (i.e. subjects) in response to the same
532 stimulus modality; (2) isolate the noise in our data by subtracting this estimate from each
533 recording; (3) *phase-randomise* each noise time-series. Phase-randomization is applied
534 independently to each node time-series in the frequency-domain. This means that the phase
535 component of the complex-valued signal is rotated at each frequency by an independent
536 random variable chosen from the uniformly distributed range of 0 and 2π (Theiler et al.,
537 1992). At the end of this process we have a new set of surrogate noise time-series.

538 To generate the full non-parametric null distribution against which to compare our data, we
539 used bootstrapping. To estimate each sample of the null distribution, we calculated the
540 differences in overall area of activation and peak amplitude, latency, position and FWHM
541 between two random sets of surrogate data without any systematic difference. To create the

13

542 random sets, we: (1) pooled together all the newly obtained surrogate noise time-series; (2)
543 added the grand average (across lance and touch) signal (as we do not want systematic
544 differences between sets to estimate a null distribution); (3) randomly split (with repetition)
545 these surrogate data into two sets. We repeated this 1000 times in order to obtain the full
546 non-parametric null distribution (bootstrapping). An experimental difference outside the 95%
547 confidence interval was considered significant (p < 0.05).

548

549 *Data sharing*
550 All raw data files are open access and are available to download from Figshare
551 (https://doi.org/10.6084/m9.figshare.13252388.v3).

552
553
554 **References**
555 Aasted CM, Yücel MA, Cooper RJ, Dubb J, Tsuzuki D, Becerra L, Petkov MP, Borsook D,
556 Dan I, Boas DA (2015) Anatomical guidance for functional near-infrared
557 spectroscopy: AtlasViewer tutorial. Neurophotonics 2:020801.
558 Akselrod M, Martuzzi R, Serino A, van der Zwaag W, Gassert R, Blanke O (2017)
559 Anatomical and functional properties of the foot and leg representation in areas 3b, 1
560 and 2 of primary somatosensory cortex in humans: A 7T fMRI study. NeuroImage
561 159:473–487.
562 Allievi AG, Arichi T, Tusor N, Kimpton J, Arulkumaran S, Counsell SJ, Edwards AD, Burdet
563 E (2016) Maturation of Sensori-Motor Functional Responses in the Preterm Brain.
564 Cereb Cortex 26:402–413.
565 Andersson JL, Lilja A, Hartvig P, Långström B, Gordh T, Handwerker H, Torebjörk E (1997)
566 Somatotopic organization along the central sulcus, for pain localization in humans, as
567 revealed by positron emission tomography. Exp Brain Res 117:192–199.
568 Andrews K, Fitzgerald M (1994) The cutaneous withdrawal reflex in human neonates:
569 sensitization, receptive fields, and the effects of contralateral stimulation. Pain 56:95–
570 101.
571 Bartocci M, Bergqvist LL, Lagercrantz H, Anand KJS (2006) Pain activates cortical areas in
572 the preterm newborn brain: Pain 122:109–117.
573 Beggs S, Torsney C, Drew LJ, Fitzgerald M (2002) The postnatal reorganization of primary
574 afferent input and dorsal horn cell receptive fields in the rat spinal cord is an activity-
575 dependent process. Eur J Neurosci 16:1249–1258.
576 Binmöller F-J, Müller CM (1992) Postnatal development of dye-coupling among astrocytes in
577 rat visual cortex. Glia 6:127–137.
578 Blake DT, Byl NN, Merzenich MM (2002) Representation of the hand in the cerebral cortex.
579 Behav Brain Res 135:179–184.
580 Brigadoi S, Aljabar P, Kuklisova-Murgasova M, Arridge SR, Cooper RJ (2014) A 4D
581 neonatal head model for diffuse optical imaging of pre-term to term infants.
582 NeuroImage 100:385–394.
583 Cai C, Fordsmann JC, Jensen SH, Gesslein B, Lønstrup M, Hald BO, Zambach SA, Brodin
584 B, Lauritzen MJ (2018) Stimulation-induced increases in cerebral blood flow and
585 local capillary vasoconstriction depend on conducted vascular responses. Proc Natl
586 Acad Sci 115:E5796–E5804.
587 Chang P, Fabrizi L, Fitzgerald M (2020) Distinct Age-Dependent C Fiber-Driven Oscillatory
588 Activity in the Rat Somatosensory Cortex. eNeuro 7.
589 Chang P, Fabrizi L, Olhede S, Fitzgerald M (2016) The Development of Nociceptive Network
590 Activity in the Somatosensory Cortex of Freely Moving Rat Pups. Cereb Cortex N Y
591 N 1991 26:4513–4523.
592 Chen LM, Dillenburger BC, Wang F, Friedman RM, Avison MJ (2011) High-resolution
593 functional magnetic resonance imaging mapping of noxious heat and tactile
594 activations along the central sulcus in New World monkeys. Pain 152:522–532.

14

595 Cornelissen L, Fabrizi L, Patten D, Worley A, Meek J, Boyd S, Slater R, Fitzgerald M (2013)
596   Postnatal Temporal, Spatial and Modality Tuning of Nociceptive Cutaneous Flexion
597   Reflexes in Human Infants. PLoS ONE 8 Available at:
598   https://www.ncbi.nlm.nih.gov/pmc/articles/PMC3790695/ [Accessed January 21,
599   2019].
600 Dall'Orso S, Steinweg J, Allievi AG, Edwards AD, Burdet E, Arichi T (2018) Somatotopic
601   Mapping of the Developing Sensorimotor Cortex in the Preterm Human Brain. Cereb
602   Cortex 28:2507–2515.
603 de Roever I, Bale G, Mitra S, Meek J, Robertson NJ, Tachtsidis I (2018) Investigation of the
604   Pattern of the Hemodynamic Response as Measured by Functional Near-Infrared
605   Spectroscopy (fNIRS) Studies in Newborns, Less Than a Month Old: A Systematic
606   Review. Front Hum Neurosci 12 Available at:
607   https://www.ncbi.nlm.nih.gov/pmc/articles/PMC6176492/ [Accessed March 2, 2020].
608 Delpy DT, Cope M, Zee P van der, Arridge S, Wray S, Wyatt J (1988) Estimation of optical
609   pathlength through tissue from direct time of flight measurement. Phys Med Biol
610   33:1433–1442.
611 Donadio A, Whitehead K, Gonzalez F, Wilhelm E, Formica D, Meek J, Fabrizi L, Burdet E
612   (2018) A novel sensor design for accurate measurement of facial somatosensation in
613   pre-term infants. PLOS ONE 13:e0207145.
614 Duerden EG, Grunau RE, Guo T, Foong J, Pearson A, Au-Young S, Lavoie R, Chakravarty
615   MM, Chau V, Synnes A, Miller SP (2018) Early Procedural Pain Is Associated with
616   Regionally-Specific Alterations in Thalamic Development in Preterm Neonates. J
617   Neurosci Off J Soc Neurosci 38:878–886.
618 Fabrizi L, Slater R, Worley A, Meek J, Boyd S, Olhede S, Fitzgerald M (2011) A shift in
619   sensory processing that enables the developing human brain to discriminate touch
620   from pain. Curr Biol 21:1552–1558.
621 Fabrizi L, Verriotis M, Williams G, Lee A, Meek J, Olhede S, Fitzgerald M (2016) Encoding of
622   mechanical nociception differs in the adult and infant brain. Sci Rep 6:28642.
623 Fitzgerald M (2005) The development of nociceptive circuits. Nat Rev Neurosci 6:507–520.
624 Fitzgerald M (2015) What do we really know about newborn infant pain? Exp Physiol
625   100:1451–1457.
626 Fujimoto K (1995) Pericyte-endothelial gap junctions in developing rat cerebral capillaries: A
627   fine structural study. Anat Rec 242:562–565.
628 Goksan S, Hartley C, Emery F, Cockrill N, Poorun R, Moultrie F, Rogers R, Campbell J,
629   Sanders M, Adams E, Clare S, Jenkinson M, Tracey I, Slater R (2015) fMRI reveals
630   neural activity overlap between adult and infant pain. eLife 4:e06356.
631 Guthrie D, Buchwald JS (1991) Significance Testing of Difference Potentials.
632   Psychophysiology 28:240–244.
633 Harding-Forrester S, Feldman DE (2018) Somatosensory maps. Handb Clin Neurol 151:73–
634   102.
635 Huppert T, Boas DA (2005) HomER: Hemodynamic evoked response NIRS data analysis
636   GUI. Available from the Photon Migration Imaging Lab. Martinos Cent Biomed
637   Imaging Available at: http://www. nmr. mgh. harvard. edu/PMI.
638 Iwasato T, Erzurumlu RS, Huerta PT, Chen DF, Sasaoka T, Ulupinar E, Tonegawa S (1997)
639   NMDA Receptor-Dependent Refinement of Somatotopic Maps. Neuron 19:1201–
640   1210.
641 Jones L, Laudiano-Dray MP, Whitehead K, Verriotis M, Meek J, Fitzgerald M, Fabrizi L
642   (2018) EEG, behavioural and physiological recordings following a painful procedure
643   in human neonates. Sci Data 5:180248.
644 Kashou NH, Dar IA, Hasenstab KA, Nahhas RW, Jadcherla SR (2016) Somatic stimulation
645   causes frontoparietal cortical changes in neonates: a functional near-infrared
646   spectroscopy study. Neurophotonics 4:011004.

15

647 Kenshalo DR, Iwata K, Sholas M, Thomas DA (2000) Response properties and organization
648   of nociceptive neurons in area 1 of monkey primary somatosensory cortex. J
649   Neurophysiol 84:719–729.
650 Kety SS, Schmidt CF (1948) The effects of altered arterial tensions of carbon dioxide and
651   oxygen on cerebral blood flow and cerebral oxygen consumption of normal young
652   men. J Clin Invest 27:484–492.
653 Koch SC, Fitzgerald M (2013) Activity-dependent development of tactile and nociceptive
654   spinal cord circuits. Ann N Y Acad Sci 1279:97–102.
655 Kozberg M, Hillman E (2016) Chapter 10 - Neurovascular coupling and energy metabolism
656   in the developing brain. In: Progress in Brain Research (Masamoto K, Hirase H,
657   Yamada K, eds), pp 213–242 New Horizons in Neurovascular Coupling: A Bridge
658   Between Brain Circulation and Neural Plasticity. Elsevier. Available at:
659   http://www.sciencedirect.com/science/article/pii/S0079612316000376   [Accessed
660   September 24, 2019].
661 Laudiano-Dray MP, Pillai Riddell R, Jones L, Iyer R, Whitehead K, Fitzgerald M, Fabrizi L,
662   Meek J (2020) Quantification of neonatal procedural pain severity: a platform for
663   estimating total pain burden in individual infants. Pain 161:1270–1277.
664 Lui F, Duzzi D, Corradini M, Serafini M, Baraldi P, Porro CA (2008) Touch or pain? Spatio-
665   temporal patterns of cortical fMRI activity following brief mechanical stimuli: Pain
666   138:362–374.
667 Mancini F, Haggard P, Iannetti GD, Longo MR, Sereno MI (2012) Fine-grained nociceptive
668   maps in primary somatosensory cortex. J Neurosci Off J Soc Neurosci 32:17155–
669   17162.
670 Meek JH, Tyszczuk L, Elwell CE, Wyatt JS (1998) Cerebral blood flow increases over the
671   first three days of life in extremely preterm neonates. Arch Dis Child - Fetal Neonatal
672   Ed 78:F33–F37.
673 Molavi B, Dumont GA (2012) Wavelet-based motion artifact removal for functional near-
674   infrared spectroscopy. Physiol Meas 33:259–270.
675 Oostenveld R, Praamstra P (2001) The five percent electrode system for high-resolution
676   EEG and ERP measurements. Clin Neurophysiol 112:713–719.
677 Penfield W, Boldrey E (1937) SOMATIC MOTOR AND SENSORY REPRESENTATION IN
678   THE CEREBRAL CORTEX OF MAN AS STUDIED BY ELECTRICAL
679   STIMULATION. Brain 60:389–443.
680 Pryds O, Greisen G (1989) Effect of PaCO2 and Haemoglobin Concentration on Day to Day
681   Variation of CBF in Preterm Neonates. Acta Paediatr 78:33–36.
682 Quast KB, Ung K, Froudarakis E, Huang L, Herman I, Addison AP, Ortiz-Guzman J,
683   Cordiner K, Saggau P, Tolias AS, Arenkiel BR (2017) Developmental broadening of
684   inhibitory sensory maps. Nat Neurosci 20:189–199.
685 Ranger M, Grunau RE (2014) Early repetitive pain in preterm infants in relation to the
686   developing brain. Pain Manag 4:57–67.
687 Schouenborg J (2008) Action-based sensory encoding in spinal sensorimotor circuits. Brain
688   Res Rev 57:111–117.
689 Schweiger M, Arridge SR (2014) The Toast++ software suite for forward and inverse
690   modeling in optical tomography. J Biomed Opt 19:040801.
691 Seelke AMH, Dooley JC, Krubitzer LA (2012) The Emergence of Somatotopic Maps of the
692   Body in S1 in Rats: The Correspondence Between Functional and Anatomical
693   Organization. PLOS ONE 7:e32322.
694 Slater R, Cantarella A, Gallella S, Worley A, Boyd S, Meek J, Fitzgerald M (2006) Cortical
695   Pain Responses in Human Infants. J Neurosci 26:3662–3666.
696 Slater R, Worley A, Fabrizi L, Roberts S, Meek J, Boyd S, Fitzgerald M (2010) Evoked
697   potentials generated by noxious stimulation in the human infant brain. Eur J Pain
698   Lond Engl 14:321–326.

16

699 Tachtsidis I, Scholkmann F (2016) False positives and false negatives in functional near-
700   infrared spectroscopy: issues, challenges, and the way forward. Neurophotonics
701   3:031405.
702 Takano T, Tian G-F, Peng W, Lou N, Libionka W, Han X, Nedergaard M (2006) Astrocyte-
703   mediated control of cerebral blood flow. Nat Neurosci 9:260–267.
704 Theiler J, Eubank S, Longtin A, Galdrikian B, Doyne Farmer J (1992) Testing for nonlinearity
705   in time series: the method of surrogate data. Phys Nonlinear Phenom 58:77–94.
706 Thivierge J-P, Marcus GF (2007) The topographic brain: from neural connectivity to
707   cognition. Trends Neurosci 30:251–259.
708 Treede RD, Kenshalo DR, Gracely RH, Jones AK (1999) The cortical representation of pain.
709   Pain 79:105–111.
710 van Drongelen W (2007) 4 - Signal Averaging. In: Signal Processing for Neuroscientists (van
711   Drongelen W, ed), pp 55–70. Burlington: Academic Press. Available at:
712   https://www.sciencedirect.com/science/article/pii/B9780123708670500048
713   [Accessed November 30, 2021].
714 Verriotis M, Chang P, Fitzgerald M, Fabrizi L (2016a) The development of the nociceptive
715   brain. Neuroscience 338:207–219.
716 Verriotis M, Fabrizi L, Lee A, Cooper RJ, Fitzgerald M, Meek J (2016b) Mapping Cortical
717   Responses to Somatosensory Stimuli in Human Infants with Simultaneous Near-
718   Infrared Spectroscopy and Event-Related Potential Recording. eNeuro
719   3:ENEURO.0026-16.2016.
720 Waldenström A, Thelin J, Thimansson E, Levinsson A, Schouenborg J (2003)
721   Developmental learning in a pain-related system: evidence for a cross-modality
722   mechanism. J Neurosci Off J Soc Neurosci 23:7719–7725.
723 Whitehead K, Laudiano-Dray P, Pressler RM, Meek J, Fabrizi L (2018) T152.
724   Somatosensory evoked delta brush activity in very pre-term infants. Clin
725   Neurophysiol 129:e60–e61.
726 Whitehead K, Papadelis C, Laudiano-Dray MP, Meek J, Fabrizi L (2019) The emergence of
727   hierarchical somatosensory processing in late prematurity. Cereb Cortex 29:2245–
728   2260.
729 Willoughby WR, Thoenes K, Bolding M (2020) Somatotopic Arrangement of the Human
730   Primary Somatosensory Cortex Derived From Functional Magnetic Resonance
731   Imaging. Front Neurosci 14:598482.
732 Worley A, Fabrizi L, Boyd S, Slater R (2012) Multi-modal pain measurements in infants. J
733   Neurosci Methods 205:252–257.
734 Wyatt JS, Cope M, Delpy DT, Zee P van der, Arridge S, Edwards AD, Reynolds EOR (1990)
735   Measurement of Optical Path Length for Cerebral Near-Infrared Spectroscopy in
736   Newborn Infants. Dev Neurosci 12:140–144.

737
738
739
740
741 **Supplements and Source Data**
742
743 **Figure 1 – Source Data 1. Significant concentration changes at each channel**
744 **following innocuous mechanical stimulation (touch) of the heel and the hand and**
745 **following heel lance**

Stimulus	Channel	Max Δ[HbO] μM	Min Δ[HbO] μM	Direction of sig. Δ	p value	Max Δ[Hb] μM	Min Δ[Hb] μM	Direction of sig. Δ	p value

17

	FTT7h	0.14 (6.8s)	-0.79 (15.9s)	↓	<.001 - .012	0.05 (0.1s)	-0.38 (7.1s)		ns
	FCC5	-0.01 (8.2s)	-0.97 (22.7s)	↓	<.001 - .010	0.27 (22.9s)	-0.42 (8.2s)	↓	<.001 - .026
	FCC3	0.03 (1.9s)	-0.61 (20.5s)	↓	<.001 - .014	0.03 (23.1s)	-1.03 (9.1s)	↓	<.001 - .012
	FCC1	0.10 (8.9s)	-0.86 (23s)	↓	<.001 - .012	0.09 (22.6s)	-0.67 (8.3s)	↓	<.001 - .011
	T7h	0.24 (5s)	-0.67 (19.9s)	↓	<.001 - .016	0.62 (3.1s)	-0.12 (28.2s)	↑	<.001 - .007
	C5h	0.60 (12s)	-0.05 (2.1s)	↑	<.001 - .011	0.03 (18s)	-0.41 (7.3s)	↓	<.001 - .014
	C3h	0.53 (5.6s)	-0.20 (25.6s)	↑	<.001 - .018	0.00 (0.1s)	-0.99 (8.2s)	↓	<.001 - .016
	C1h	-0.18 (15.2s)	-0.62 (22.2s)	↓	<.001 - .012	0.39 (27.9s)	-0.47 (10.9s)	↑/↓	<.001 - .021
Heel lance	C2h	0.31 (12.8s)	-0.58 (30s)	↓	<.001 - .013	0.68 (4.4s)	-0.13 (18.5s)	↑	<.001 - .013
	CCP5	0.31 (7.2s)	-0.36 (16.4s)		ns	0.62 (2.9s)	-0.02 (26.3s)	↑	<.001 - .033
	CCP3	0.94 (14.4s)	-0.11 (2.7s)	↑	<.001 - .018	0.13 (22.9s)	-0.35 (11s)	↓	<.001 - .021
	CCP1	0.62 (8.2s)	-0.25 (29.6s)	↑	<.001 - .018	0.04 (17.8s)	-0.61 (11.3s)	↓	<.001 - .011
	CP3h	0.96 (14.5s)	-0.45 (28s)	↑	<.001 - .012	0.01 (30s)	-0.56 (9.7s)	↓	<.001 - .057
	CP1h	0.71 (15.7s)	0.02 (2.6s)	↑	<.001 - .016	0.00 (30s)	-0.39 (13s)	↓	<.001 - .022
	CP2h	0.46 (17s)	0.10 (0.1s)		ns	0.72 (20.7s)	0.12 (0.9s)	↑	<.001 - .010
	CPP1	0.91 (14.1s)	-0.39 (29.3s)	↑	<.001 - .010	0.44 (5s)	-0.12 (12.2s)	↑	<.001 - .012
	P7	0.52 (12.1s)	-0.19 (24.3s)	↑	<.001 - .011	0.28 (23.6s)	-0.12 (14.2s)	↑	<.001 - .025
	FTT7h	0.08 (7s)	-0.26 (30s)	↓	<.001 - .016	0.12 (26.9s)	-0.09 (12s)	↑/↓	<.001 - .020
	FCC5	0.09 (5.7s)	-0.11 (30s)		ns	0.12 (30s)	-0.02 (8.3s)	↑	<.001 - .015
	FCC3	0.06 (2.6s)	-0.17 (15.1s)	↓	<.001 - .038	0.08 (30s)	-0.21 (11.1s)	↓	<.001 - .014
	FCC1	0.01 (8.1s)	-0.14 (24.4s)	↓	<.001 - .013	0.05 (30s)	-0.17 (11.1s)	↓	<.001 - .013
Heel touch	T7h	0.07 (10.6s)	-0.09 (30s)		ns	0.04 (28.2s)	-0.05 (13.1s)		ns
	C5h	0.07 (9.2s)	-0.02 (28.3s)		ns	0.03 (30s)	-0.12 (11.1s)	↓	<.001 - .022
	C3h	0.03 (1.1s)	-0.16 (24.3s)	↓	<.001 - .011	0 (24.8s)	-0.15 (11.3s)	↓	<.001 - .021
	C1h	0.2 (14.2s)	-0.1 (24.3s)	↑	<.001 - .014	0.06 (30s)	-0.14 (9.7s)	↓	<.001 - .013
	C2h	0.19 (9.2s)	-0.1 (30s)	↑	<.001 - .016	0.08 (24.9s)	-0.1 (12.3s)	↓	<.001 - .013

	CCP5	0.06 (10.4s)	-0.11 (28.7s)	↓	<.001 - .010	0.11 (28.1s)	-0.08 (11.3s)	↑/↓	<.001 - .014
	CCP3	0.02 (9.2s)	-0.08 (25s)		Ns	0.1 (24.7s)	-0.09 (9.6s)	↑/↓	<.001 - .016
	CCP1	0.15 (14.3s)	0 (24.4s)	↑	<.001 - .011	0.04 (4.2s)	-0.07 (23.8s)	↓	<.001 - .019
	CP3h	0.12 (13.5s)	-0.05 (5.2s)	↑	<.001 - .011	0.06 (4.4s)	-0.13 (13.7s)	↓	<.001 - .011
	CP1h	0.23 (14.9s)	0 (30s)	↑	<.001 - .018	0.07 (4.1s)	-0.1 (25.4s)	↓	<.001 - .010
	CP2h	0.04 (9s)	-0.09 (26.9s)		Ns	0.02 (4.7s)	-0.16 (28s)	↓	<.001 - .029
	CPP1	0.35 (15.8s)	0.03 (0.1s)	↑	<.001 - .023	0.08 (14.9s)	-0.01 (29.5s)	↑	ns
	P7	0.14 (16.8s)	-0.11 (30s)	↑	<.001 - .013	0.09 (19.9s)	-0.09 (9.1s)	↑/↓	<.001 - .012
	FTT7h	0.29 (11.4s)	-0.07 (23.4s)	↑	<.001 - .012	0.06 (26.1s)	-0.08 (3.4s)		ns
	FCC5	0.33 (9.2s)	0.02 (1s)	↑	<.001 - .025	0.05 (30s)	-0.14 (8.8s)	↓	<.001 - .011
	FCC3	0.27 (17.1s)	-0.09 (1s)	↑	<.001 - .019	0.04 (30s)	-0.15 (11.5s)		ns
	FCC1	0.17 (19s)	-0.01 (6s)	↑	<.001 - .012	-0.02 (7.2s)	-0.18 (17.6s)	↓	<.001 - .018
	T7h	0.05 (30s)	-0.1 (4.8s)		ns	0.17 (4.7s)	-0.04 (14.8s)		ns
	C5h	0.2 (9.5s)	-0.04 (29.8s)	↑	<.001 - .011	0.09 (30s)	-0.11 (11.2s)	↓	<.001 - .010
	C3h	0.05 (16.5s)	-0.17 (30s)	↓	<.001 - .010	0.13 (29.2s)	-0.06 (0.9s)	↑	<.001 - .013
	C1h	0.19 (11.3s)	-0.13 (24.2s)		ns	0.12 (23.9s)	-0.15 (11.7s)	↓	<.001 - .010
Hand touch	C2h	0.08 (2.5s)	-0.29 (28.9s)	↓	<.001 - .011	0.19 (24.2s)	-0.11 (6.2s)	↑	<.001 - .015
	CCP5	0.06 (15.7s)	-0.11 (7.6s)		ns	0.03 (23s)	-0.07 (15.1s)		ns
	CCP3	0.12 (5.5s)	-0.15 (30s)	↑/↓	<.001 - .016	0.11 (26.7s)	-0.14 (9.5s)	↓	<.001 - .013
	CCP1	0.1 (3s)	-0.15 (26.9s)	↓	<.001 - .013	0.12 (30s)	-0.09 (8.6s)	↑	<.001 - .017
	CP3h	0.09 (3s)	-0.21 (20.4s)	↓	<.001 - .015	0.08 (27.9s)	-0.14 (10.1s)	↓	<.001 - .025
	CP1h	0.14 (3.1s)	-0.11 (23.5s)		ns	0.02 (29s)	-0.13 (6.4s)	↓	<.001 - .020
	CP2h	0.11 (2.4s)	-0.15 (16.7s)		ns	0.13 (24.9s)	-0.01 (10.2s)	↑	<.001 - .034
	CPP1	0.07 (1.4s)	-0.04 (8.4s)		ns	-0.03 (1.7s)	-0.14 (16.1s)	↓	<.001 - .017
	P7	0.13 (27s)	-0.05 (17.2s)	↑	<.001 - .013	0.05 (26.7s)	-0.03 (18.6s)		ns

746 *Minimum and maximum Δ[HbO] and Δ[Hb] at every channel and the corresponding latency.*
747 *The range of Bonferroni-corrected p values across all significant timepoints is provided. ↓ =*

significant decrease only, ↑ significant increase only, ↑/↓ = both a significant increase and
749 *decrease were observed at different latencies. Channel names are according to the 10-5*
750 *placement system. The location of each channel is shown in Figure 4.*
751
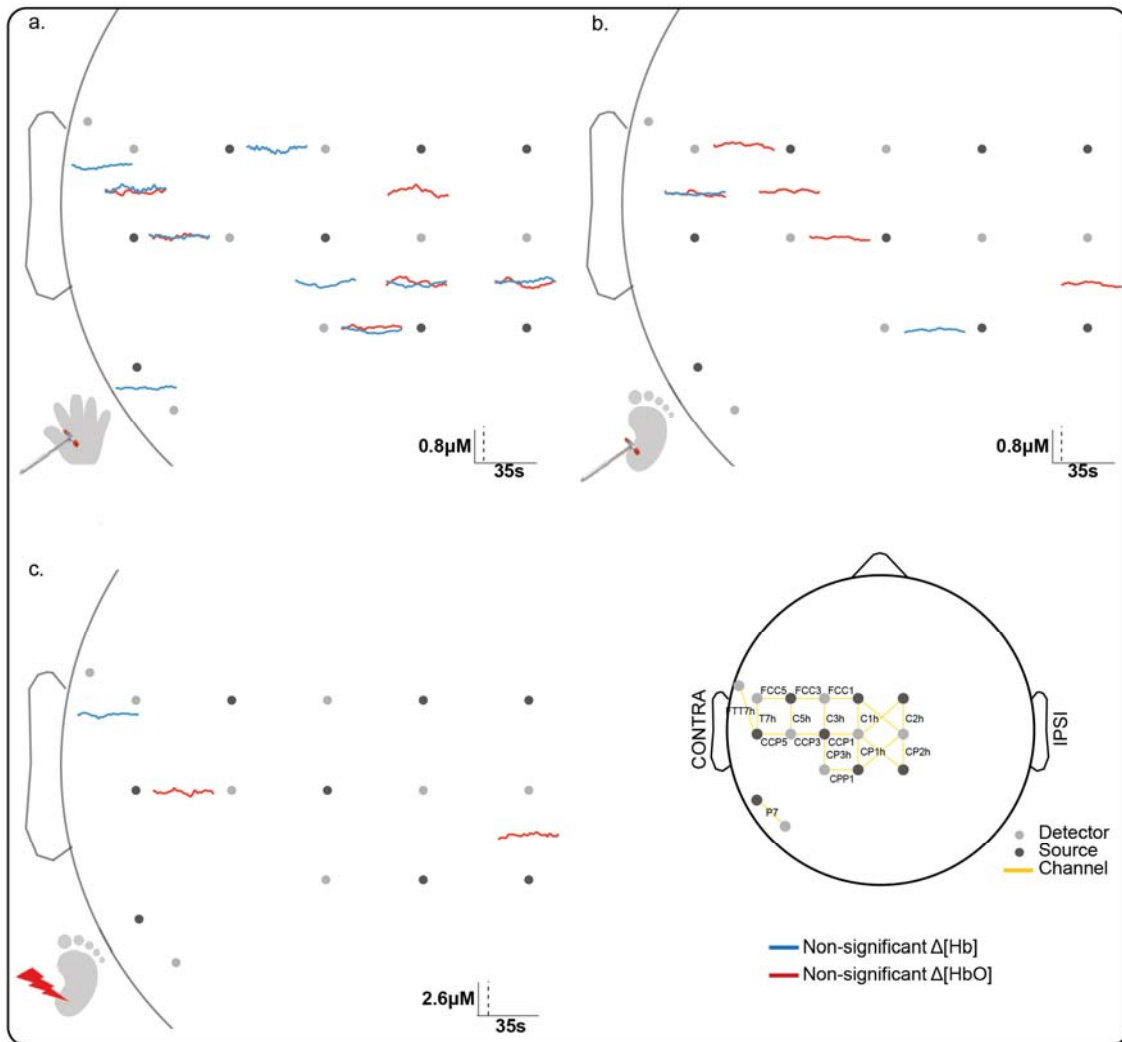
752
753 **Figure 1 - figure supplement 1.**
754 **Non-significant channel-wise haemodynamic responses following innocuous and**
755 **noxious mechanical stimulation of hand and heel.** *Average non-significant change in*
756 concentration of oxygenated *(Δ[HbO]) (red) and deoxygenated haemoglobin (Δ[Hb]) (blue)*
757 *during (a) hand touch (n=11), (b) heel touch (n=16) and (c) heel lance (n=11). Channels with*
758 *increases in [HbO] and decreases in [Hb] (i.e. canonical response) during the activation*
759 *period are shown with sold dark lines, inverse responses are shown with solid pale lines.*
760 *Black vertical line represents stimulus onset. Note the difference in the scale bar between*
761 *touch and lance. For channels where a non-significant canonical and inverse response was*
762 *found at different latencies, the canonical response only is depicted.*
763

20

764
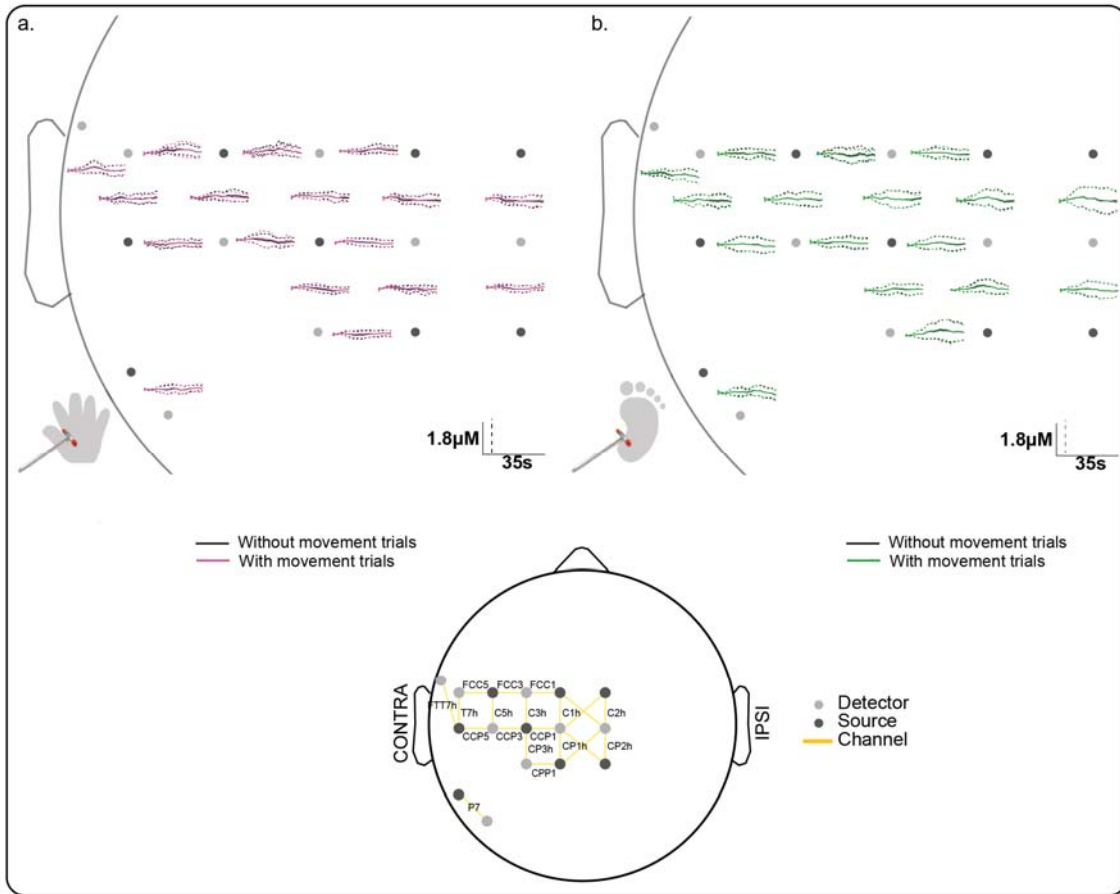
Figure 1 - figure supplement 2.

Average channel-wise Δ[HbO] response following innocuous mechanical stimulation of the hand and heel with and without excluding trials with movement. *Average change in concentration of oxygenated (Δ[HbO]) haemoglobin during (a) hand touch (n=11) and (b) heel touch (n=16) with (pink/green) and without (black) trials during which the infant moved. Dashed lines represent standard deviation. No significant differences were found at any channel.*

772

21
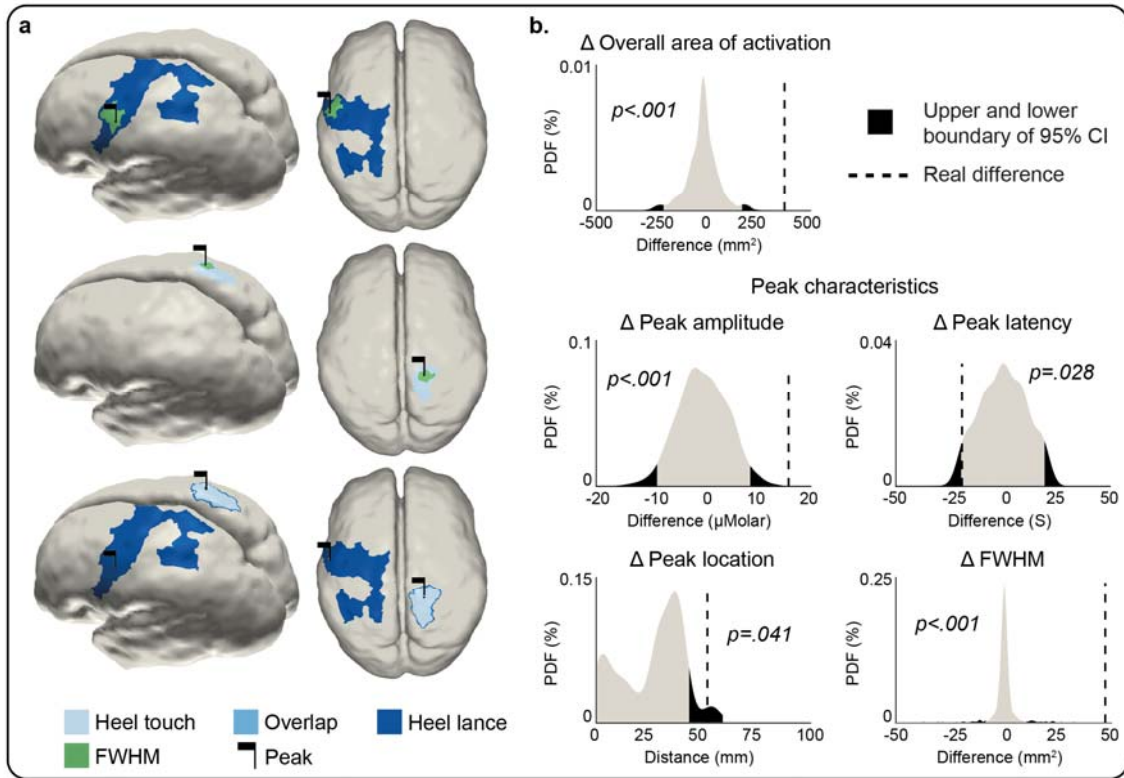
773
774 **Figure 3 – figure supplement 1.**
775 **Comparison of the peak and area of activation of the Δ[Hb] response to an innocuous**
776 **(touch) and noxious (lance) mechanical stimulation of the heel.** (*a) Overall area of*
777 *significant changes in concentration of deoxygenated haemoglobin (Δ[Hb]) following heel*
778 *lance (dark blue), heel touch (pale blue) and both (mid blue). Black flags demark the location*
779 *of peak changes and green areas the extent of their full-width half-maximum (FWHM). (b)*
780 *Statistical position of real differences between heel touch and lance in peak amplitude,*
781 *FWHM, latency and location, and overall area of activation in respect to non-parametric null*
782 *distributions obtained with bootstrapping and phase scrambling.*
783
784
785 **Figure 3 – Source Data 1.**
786 **Comparison of Δ[HbO] and Δ[Hb] responses to an innocuous (touch) and noxious**
787 **(lance) mechanical stimulation of the heel.** Parameter estimates for the change in
788 oxygenated haemoglobin (Δ[HbO]) and deoxygenated haemoglobin (Δ[Hb]) following a heel
789 lance and heel touch, and p value from statistical comparison. A two-tailed test was used
790 (alpha = .025) for all parameters except peak location (alpha = .05). The Euclidean distance
791 between the heel touch and heel lance peak locations has been provided rather than x,y,z
792 coordinates of each peak. Linked to Figure 3 and Supplementary Figure 1.

	Δ[HbO]			Δ[Hb]		
Parameter	Lance	Heel touch	p value	Lance	Heel touch	p value
Overall area (mm²)	455.27	259.51	.009	475.24	95.53	<.001
Peak amplitude (µM)	16.06	5.43	.001	-22.54	-6.62	<.001
Peak latency (s)	14	16	.358	9.5	28	.028
Peak location (mm)	Euclidean distance = 1.65		.156	Euclidean distance = 51.88		.041
Peak spread (mm²)	51.41	43.79	.019	15.31	4.63	<.001

22

793